Dissecting and Targeting the Growth Factor–Dependent and Growth Factor–Independent Extracellular Signal-Regulated Kinase Pathway in Human Schwannoma

Sylwia Ammoun,[1] Christine Flaiz,[1] Natalia Ristic,[1] Jennifer Schuldt,[2] and C. Oliver Hanemann[1]

[1]Clinical Neurobiology, Peninsula College for Medicine and Dentistry, Plymouth, United Kingdom; and [2]Department of Neurology, Zentrum fuer Klinische Forschung, University of Ulm, Ulm, Germany

Abstract

Schwannomas are tumors of the nervous system that occur sporadically and in patients with the cancer predisposition syndrome neurofibromatosis type 2 (NF2). Schwannomas and all NF2-related tumors are caused by loss of the tumor suppressor merlin. Using our human *in vitro* model for schwannoma, we analyzed extracellular signal-regulated kinase 1/2 (ERK1/2) and AKT signaling pathways, their upstream growth factor receptors, and their role in schwannoma cell proliferation and adhesion to find new systemic therapies for these tumors that, to date, are very difficult to treat. We show here that human primary schwannoma cells show an enhanced basal Raf/mitogen-activated protein/ERK kinase/ERK1/2 pathway activity compared with healthy Schwann cells. Due to a strong and prolonged activation of platelet-derived growth factor receptor β (PDGFRβ), which is highly overexpressed, ERK1/2 and AKT activation was further increased in schwannoma, leading to increased proliferation. Using specific inhibitors, we discovered that ERK1/2 activation involves the integrin/focal adhesion kinase/Src/Ras signaling cascades and PDGFRβ-mediated ERK1/2 activation is triggered through the phosphatidylinositol 3-kinase/protein kinase C/Src/c-Raf pathway. Due to the complexity of signals leading to schwannoma cell proliferation, potential new therapeutic agents should target several signaling pathways. The PDGFR and c-Raf inhibitor sorafenib (BAY 43-9006; Bayer Pharmaceuticals), currently approved for treatment of advanced renal cell cancer, inhibits both basal and PDGFRβ-mediated ERK1/2 and AKT activity and decreases cell proliferation in human schwannoma cells, suggesting that this drug constitutes a promising tool to treat schwannomas. We conclude that our schwannoma *in vitro* model can be used to screen for new therapeutic targets in general and that sorafenib is possible candidate for future clinical trials. [Cancer Res 2008;68(13):5236–45]

Introduction

Schwannomas are common tumors of the nervous system occurring sporadically and in patients with the inherited cancer predisposition syndrome neurofibromatosis type 2 (NF2). Schwannomas are purely derived from Schwann cells and lack the tumor suppressor protein merlin (1). Merlin is structurally related to the ERM family proteins (ezrin, moesin and radixin; refs. 2, 3) that act as linkers between the actin cytoskeleton and the cell membrane (4). Using our *in vitro* model for human schwannoma, we have previously shown that merlin loss leads to enhanced proliferation and decreased apoptosis (5), increased cell-matrix adhesion (due to the overexpression of integrins; ref. 6), and decreased cell-cell adhesion (7). The RhoGTPases Rac1 and Cdc42 and their downstream effector p21-activated kinase (PAK) are activated in human primary schwannoma cells and have been linked to the aforementioned characteristics of schwannoma cells (8, 9). PAK inhibits merlin in a negative feedback loop (10, 11), and PAK inhibition leads to decreased proliferation rates and ruffling in merlin-deficient cell lines (12). PAK can cross-talk with the extracellular signal-regulated kinase 1/2 (ERK1/2) signaling pathway. The ERK1/2 signaling pathway is involved in rat Schwann cell dedifferentiation (13), integrin-mediated cell motility, adhesion (14), and proliferation (15). ERK1/2 that is activated in mouse and rat schwannoma cell lines (16) is inhibited by merlin in different cell lines (17). We therefore analyzed ERK1/2 pathway in human primary schwannomas and assessed its role in cell proliferation and adhesion to identify potential therapeutic targets for the treatment of schwannomas. Merlin additionally inhibits the AKT signaling pathway (18, 19), which is important for rat Schwann cell survival (20).

Activation of ERK1/2 and AKT cascades is triggered by surface receptors, such as integrins and receptor tyrosine kinases (21). One candidate is platelet-derived growth factor receptor β (PDGFRβ), wherein internalization and degradation is merlin-dependent in human schwannoma cell line HEI 193 (18). Moreover, PDGFRβ interacts directly with integrins (22), which are overexpressed in human primary schwannoma cells (6). We thus investigated the role of PDGFRβ and other growth factor receptors acting upstream of the ERK1/2 and AKT pathways in human primary schwannoma cells. We show that ERK1/2 and subsequent enhanced proliferation occur through a strong and prolonged activation of PDGFRβ after stimulation of human primary schwannoma cells with the PDGFRβ-specific agonist, platelet-derived growth factor-DD (PDGF-DD). In addition, schwannoma cells display an enhanced basal ERK1/2 activity compared with Schwann cells. Strong AKT activity was also observed in schwannoma cells upon stimulation with PDGF-DD. Using specific inhibitors, we characterized the mechanisms of ERK1/2 and AKT activation. Basal ERK1/2 activation involves the integrin/focal adhesion kinase (FAK)/Src/Ras signaling cascade, and PDGFRβ-mediated ERK1/2 activation involves the phosphatidylinositol 3-kinase (PI3K)/protein kinase C (PKC)/Src/c-Raf pathway. Cross-talk between ERK1/2 and AKT cascades was also observed. Based on our data, we conclude that

Note: Supplementary data for this article are available at Cancer Research Online (http://cancerres.aacrjournals.org/).

Requests for reprints: C. Oliver Hanemann, Clinical Neurobiology, Peninsula College for Medicine and Dentistry, The John Bull Building, Tamar Science Park, Research Way, Plymouth PL6 8BU, United Kingdom. Phone: 44-1752-437-418; Fax: 44-1752-517-846; E-mail: oliver.hanemann@pms.ac.uk.

doi:10.1158/0008-5472.CAN-07-5849

multiple cascades underlie schwannoma development and therefore suggest that potential therapeutic agents should target several signaling pathways. We therefore tested the PDGFR and c-Raf inhibitor sorafenib (BAY 43-9006; Bayer Pharmaceuticals), currently approved for the treatment of advanced renal cell cancer (RCC; ref. 23). We here show that sorafenib inhibits both basal and PDGFRβ-mediated ERK1/2 and AKT activity and decreases proliferation of human schwannoma cells, suggesting that this drug could be a useful tool in the treatment of schwannomas.

Materials and Methods

Isolation and culture of human Schwann and schwannoma cells. Human Schwann cells from healthy nerve donors and schwannoma cells from patients with NF2 (after informed consent) were isolated, as previously described (24, 25). Diagnosis of NF2 was established by clinical criteria (26). Cell were harvested and resuspended in proliferation medium (GFM): DMEM, 10% FCS, 0.5 μmol/L forskolin, 10 nmol/L β heregulin, 0.5 mmol/L 3-isobutyl-1-methylxanthine (IBMX), and 2.5 μg/mL insulin, as described in ref. 25.

Chemicals. GF109203X, LY294002, SU6656, U0126 (kindly supplied by Prof. Jyrki Kukkonen, University of Helsinki), IPA-3 (kindly supplied by Dr. Jeffrey R Peterson, Fox Chase Cancer Center), AG1296, 5-bromo-2′-deoxyuridine (BrdUrd) and FTI-277 were from Calbiochem. 12-*O*-tetradecanoylphorbol-13-acetate (TPA), GW5074, *t*-octylphenoxypolyethoxyethanol (Triton X-100), polyoxyethylene sorbitan monolaurate (Tween 20), insulin, and IBMX were from Sigma. Wortmannin (kindly supplied by Prof. Jyrki Kukkonen, University of Helsinki) was from Tocris Cookson Ltd., PDGF-DD from R&D Systems. Hoechst 33352 was from Molecular Probes (Eugene), and sorafenib (BAY 43-9006) was kindly supplied by Bayer Pharmaceuticals (West Haven). All inhibitors were added 30 min before PDGF-DD stimulation.

Immunoblotting. Cells were cultured in precoated 35-mm plates to ~70% confluency, serum-starved for 24 h, stimulated, and lysed (5). The immunoblotting was performed, as described in refs. 8, 9. Membranes were incubated with antiactive mitogen-activated protein kinase (MAPK; anti-pThr^{183}-pTyr^{185}-ERK1/2; 1:2,000; Promega), anti–phosphorylated AKT (Ser^{473}; 1:500; Cell Signaling), anti–phosphorylated MAPK/ERK kinase 1/2 (MEK1/2) (Ser^{298}; 1:500; Cell Signaling), anti–phosphorylated MEK1/2 (Ser$^{217/221}$; 1:500; Cell Signaling), anti–phosphorylated c-Raf (Ser^{338}; 1:500; Cell Signaling), anti–phosphorylated FAK (p-FAK; Y^{925}; 1:500; Cell Signaling), anti–p-FAK (Y^{861}; 1:500; Stressgen), and anti–p-FAK (Y^{397}; 1:200: Chemicon) primary antibodies, followed by incubation with appropriate horseradish peroxidase–conjugated secondary antibodies (Bio-Rad). Enhanced chemiluminescence (Amersham) was used for detection. RhoGDI was used as a loading control, as it has previously been shown not to be regulated in our system (27) in contrast to standard loading controls. Densities of bands were quantified using FluorS-Multi-Imager (Bio-Rad). After stripping and blocking total ERK, MEK, FAK, and AKT levels were determined using anti–total MAPK (ERK1/2, 1:500; Promega), MEK1/2 (1:500; Cell Signaling), FAK (1:500; Upstate), and AKT (1:500; Cell Signaling) antibodies. The expression levels of PDGFRβ, epidermal growth factor (EGF) receptor (EGFR), ErbB2, and ErbB3 were detected using anti-PDGFRβ (1:500) and anti-EGFR (1:500; Cell Signaling), anti-ErbB2 (NeuC18; 1:1000), and anti-ErbB3 (1:1000) antibodies from Santa Cruz Biotechnology.

Ras pull-down. Cells were grown until ~70% confluence, starved for 24 h, stimulated with 100 ng/mL of PDGF-DD for 3 min in the presence or absence of the Ras inhibitor FTI-277 and lysed. Ras pull-down experiments were performed using the EZ-Detect Ras activation kit (Promega) according to manufacturer's protocol. Western blotting was performed, as described above, using an anti-Ras antibody (1:500; Promega).

Immunocytochemistry. Cells were serum starved for 24 h before stimulation, and immunocytochemistry was performed, as described in refs. 8, 9. Anti–active MAPK (anti-pThr^{183}-pTyr^{185}-ERK1/2; 1:2,000; Promega) and anti–p-FAK Y^{397} antibodies were used for detection of active ERK1/2 and FAK, respectively. Appropriate Cy3 or ALEXA Fluor 488–labeled secondary antibodies were used (1:500; Sigma).

Adhesion assay. Cells were seeded onto precoated 24-well plates for 3 h (28) using different conditions: DMEM, 100 ng/mL PDGF-DD, and GFM. Adhesion assay was performed as described (6).

BrdUrd incorporation and nuclear staining for cell growth. Cells were cultivated on 96-well plates (Nunc) for 72 h, labeled with 10 μmol/L BrdUrd for 24 h, fixed with 4% paraformaldehyde, and incubated with 2 mol/L HCl. Cells were blocked in 2% (w/v) bovine serum albumin and incubated with anti-BrdUrd (1:100; Calbiochem) followed by ALEXA Fluor 488–labeled secondary antibody (1:500; Molecular Probes). Nuclei were stained with 5 μg/mL Hoechst 33342 for 30 min. Dividing cells (BrdUrd positive) and total cell numbers (Hoechst 33342) were manually counted. All inhibitors were added 30 min before stimulation.

Data analysis. Student's two-tailed *t* test was used for pairwise comparisons and ANOVA, followed by Tukey's post hoc test, was used for multiple comparisons. All the experiments were performed minimum in triplicates, wherein at least three independent batches of cells from different individuals were used. For cell counting, all cells in the well were counted. ns means (not significant) $P > 0.05$, * indicates $P < 0.05$; ** indicates $P < 0.01$, and *** indicates $P < 0.001$. Significant values are indicated only for the data in which the results are not self-evident. In figures, mean ± SE is given.

Results

Strong Activation of ERK1/2 in Human Primary Schwannoma Cells

Incubation of serum-starved cells with complete medium (GFM) for 10 minutes, 3 hours, and 24 hours produced a higher phosphorylation/activation intensity of ERK1/2 in schwannoma cells compared with Schwann cells (Fig. 1*A*). In addition to bands at 42/44 kDa, we also observed weak but specific bands (confirmed by library searches of the recognized epitope using Phospho.ELM screening) at ~300 kDa, which displayed the same pattern of activity as the lower molecular weight bands. The data in Fig. 1*A* represent total ERK1/2 activity in cells (combined data of 42/44 kDa and 300 kDa bands). Maximal phosphorylation of ERK1/2 occurred in both cell types 10 minutes poststimulation and was 3-fold higher in schwannoma cells than in Schwann cells. Furthermore, we stimulated schwannoma cells with various components present in GFM and observed that serum phosphorylated ERK1/2 to the levels comparable with GFM, whereas insulin, forskolin, IBMX, and β-heregulin evoked only weak to moderate signals even when used at high concentrations (Fig. 1*B* and *C*). Stimulation of schwannoma cells with 100 ng/mL PDGF-DD increased levels of phosphorylated ERK1/2 by 7-fold compared with basal, the same magnitude as serum and GFM (Fig. 1*B* and *C*). 100 ng/mL of EGF and fibroblast growth factor acidic (FGFa), whose functionality was tested in NIH3T3 and PC12 cells, did not trigger ERK1/2 activation in schwannoma cells (Fig. 1*C*). In line with this, schwannoma cells show no expression of EGFR (Supplementary Fig. S1). Moreover, Schwann and schwannoma cells express similar levels of ErbB2 and ErbB3 receptors (Fig. 1*D*) and β heregulin even at high concentrations (100 nmol/L) displayed much lower potency toward ERK1/2 activation than PDGF-DD (100 ng/mL; Fig. 1*B* and *C*).

PDGFRβ Activation Leads to Strong and Sustained Activation of MEK1/2 and ERK1/2 in Schwannoma Cells

PDGF-DD (100 ng/mL) induced strong and long-lasting MEK1/2 and ERK1/2 activity in schwannoma cells (Fig. 2*A*). As with GFM, in addition to 42/44 kDa bands, specific phosphorylated ERK1/2 (p-ERK1/2) bands were also observed at 300 kDa. The 300-kDa

bands were stronger upon PDGF-DD stimulation than upon GFM stimulation and displayed higher ERK1/2 activity in schwannoma cells compared with Schwann cells already 10 minutes after stimulation in contrast to 42/44 kDa bands where the significant difference was seen only after 1 hour (Fig. 2*A*, compare *rows 2* and *3, top*). The specificity of 300-kDa bands was estimated by Phospho.ELM screening and by using 2 μmol/L TPA. Despite strong ERK1/2 activity at 42/44 kDa, no band at 300 kDa was observed upon TPA stimulation, suggesting that 300 kDa bands are specific for PDGF-DD stimulation (Fig. 2*B*). Thus, to show total ERK activity in cells, Fig. 2*A* (*bottom*) shows combined data from 42/44 kDa and 300 kDa bands. Maximal MEK1/2/ERK1/2 phosphorylation occurred 10 minutes after stimulation and persisted at least up to 1 hour at 60% to 70% (MEK1/2) and 40% (ERK1/2) of maximal response and declined to basal levels after 24 hours. In comparison, Schwann cells displayed a weaker and only transient activity, which declined to almost basal levels already within 1 hour after stimulation.

AKT is Strongly Activated in Schwannoma Cells upon PDGFRβ Stimulation

AKT showed strong and sustained phosphorylation/activation at Ser^{473} in schwannoma cells upon stimulation with 100 ng/mL PDGF-DD (Fig. 2*C*) and was observed only at its expected molecular weight size (60 kDa).

Maximal activity was reached 10 minutes poststimulation and remained higher than basal up to 24 hours. Schwann cells in contrast displayed much weaker (maximal response was approximately twice lower than in schwannoma cells) and transient AKT activity, which decreased to basal levels at already 1 hour poststimulation. Total MEK1/2, ERK1/2, and AKT expression remained unchanged during all this conditions, and no difference between schwannoma and Schwann cells was detected (Fig. 2*A*, *middle* and *bottom* and Fig. 2*C*, *bottom*).

PDGFRβ is Overexpressed in Schwannoma Cells

PDGFRβ is overexpressed in schwannoma cells (~2-fold) compared with Schwann cells (Fig. 3*A*). Also, schwannoma cells display postponed and impaired PDGFRβ degradation as its levels were decreased only by ~35% within 1 hour of stimulation and by ~65% after 24 hours (Fig. 3*B*) in contrast to Schwann cells where the decrease was more pronounced (~85%; Fig. 3*C* and *D*). The decrease in PDGFRβ phosphorylation was slightly faster than its degradation: it decreased by ~50% (from maximum) 1 hour after stimulation and was abolished 24 hours poststimulation (Fig. 3*B*) following the same pattern as phosphorylated MEK1/2 (p-MEK1/2) and p-ERK1/2 activation course (see Fig. 2*C*, *middle* and *bottom*).

A PDGFRβ-Independent Pathway Contributes to ERK1/2 Activation in Schwannoma Cells

In addition to PDGF-DD mediated MEK1/2 and ERK1/2 activation, our data (Fig. 2*A*; 0 hours) also shows increased basal levels of phosphorylated MEK1/2 and ERK1/2 in schwannoma cells

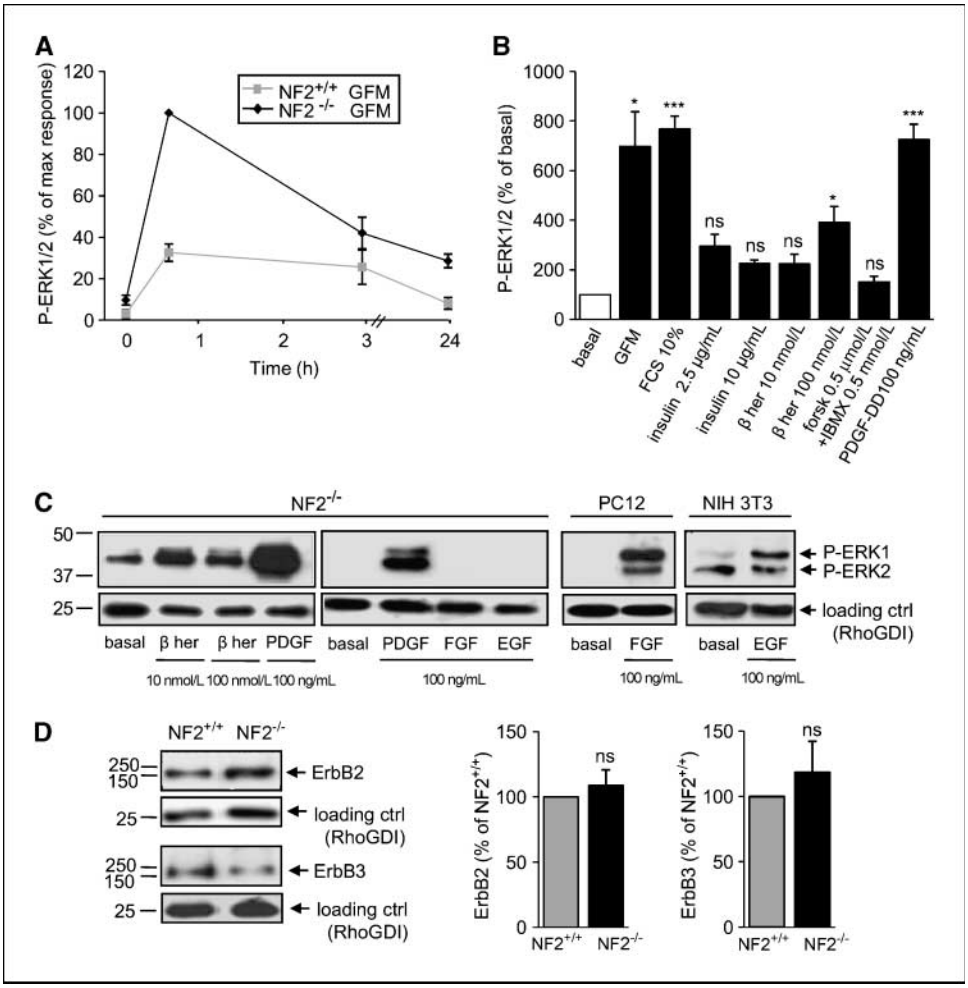

Figure 1. The role of PDGFRβ in schwannoma cell signaling. *A,* schwannoma cells display strong and long-lasting ERK1/2 activation compared with Schwann cells. Time-response curves for ERK1/2 activation upon GFM (complete medium) stimulation in Schwann ($NF2^{+/+}$) and schwannoma ($NF2^{-/-}$) cells. *B* and *C,* PDGF-DD is a potent ERK1/2 activator in schwannoma cells. *B,* ERK1/2 phosphorylation in schwannoma cells after 10 min stimulation with GFM, FCS, insulin, β heregulin, forskolin, IBMX, and PDGF-DD. *C,* ERK1/2 phosphorylation after 10 min stimulation of schwannoma cells with β heregulin, PDGF-DD, FGFa, and EGF and PC12 and NIH3T3 cells with FGFa and EGF, respectively. *D,* ErbB2 and ErbB3 are equally expressed in Schwann and schwannoma cells. In all experiments but *D*, cells were starved for 24 h before the stimulation. The phosphorylated/activated levels of ERK1/2 and receptor expression were detected by Western blot. *A,* data are normalized to maximum GFM stimulation (100%). *B,* data are normalized to the basal level (nonstimulated cells). *D,* data are normalized to $NF2^{+/+}$. All data are corrected to loading control RhoGDI. In *A*, the error bars at 0 and 10 min time point for $NF2^{+/+}$ are not visible because of very low SD.

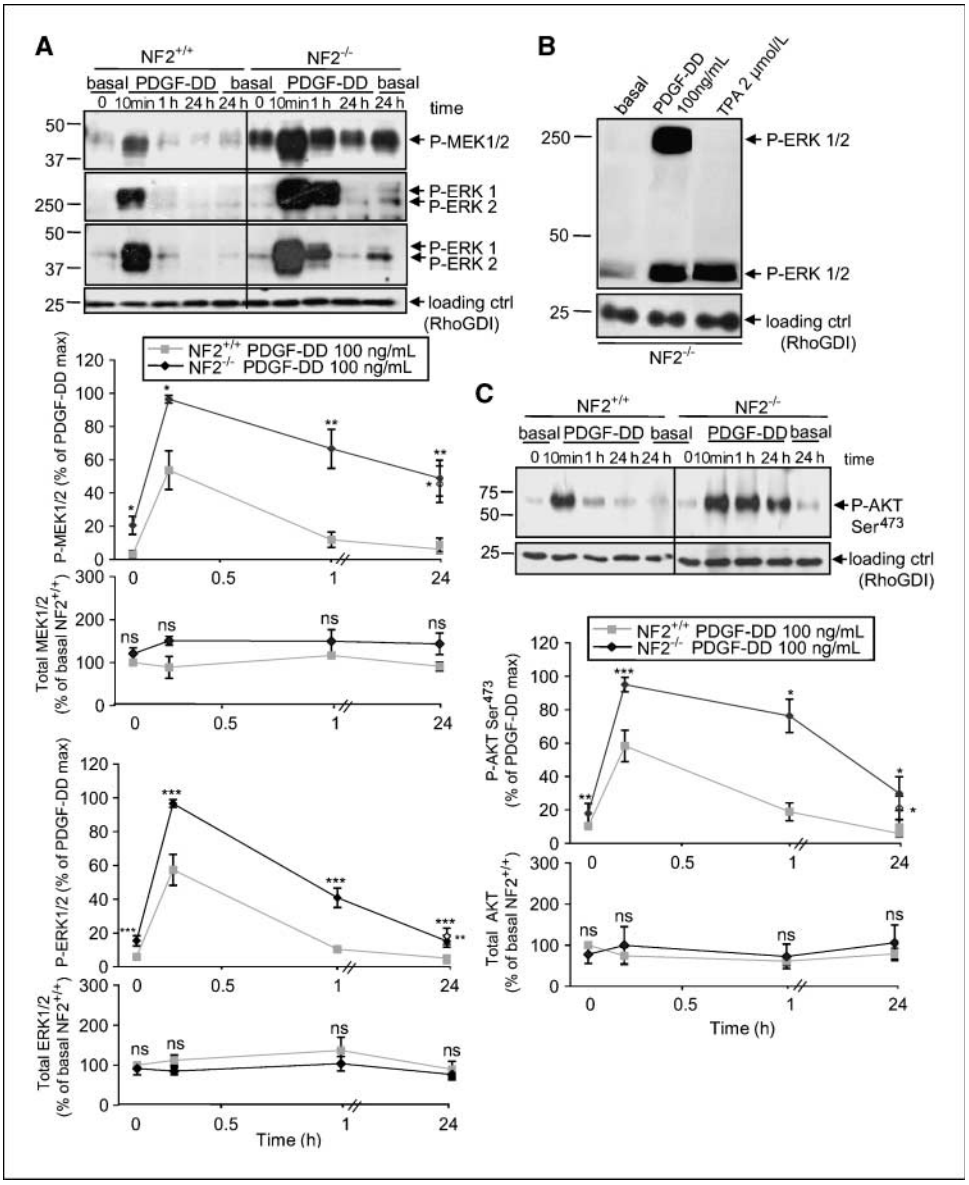

Figure 2. Time-response curves for MEK1/2, ERK1/2, and AKT phosphorylation. *A* and *C,* schwannoma cells display strong and long-lasting activation of MEK1/2, ERK1/2, and AKT. Schwann ($NF2^{+/+}$) and schwannoma cells ($NF2^{-/-}$) were starved for 24 h and stimulated for the time indicated with PDGF-DD (100 ng/mL). MEK1/2 (*A, top* and *middle*), ERK1/2 (*A, top* and *bottom*), and AKT (*C*) phosphorylation/activation was assessed by Western blot. *A, top* and *B,* upon PDGF-DD stimulation of ERK1/2, specific bands at 300 kDa (in addition to 42/44 kDa) are observed. TPA (2 μmol/L, 10 min) activates ERK1/2 only at the 42/44 kDa level. *A* (*middle* and *bottom*) and *C* (*bottom*), the expression of MEK1/2, ERK1/2, and AKT remains unchanged during PDGF-DD stimulation and displays no difference between Schwann and schwannoma cells. Cells were starved for 24 h and stimulated for the time indicated with PDGF-DD (100 ng/mL). The expression of MEK1/2, ERK1/2, and AKT was assessed by Western blot. In *A* (*bottom*; p-MEK1/2 and p-ERK1/2) and *C* (*bottom*; p-AKT), the data are normalized to the maximum PDGF-DD stimulation (100%), and in *A* (*bottom*; total MEK1/2 and total ERK1/2) and *C* (*bottom*; total AKT), the data are normalized to basal $NF2^{+/+}$. *Empty squares* (*A, middle* and *bottom* and *C, bottom*), basal levels for 24 h stimulation. All data are corrected to loading control RhoGDI.

compared with Schwann cells. Because both MEK1/2 and ERK1/2 are equally expressed in Schwann and schwannoma cells (see Fig. 2*A*), we can exclude MEK1/2 and ERK1/2 overexpression as a reason for enhanced activity and tested the following possibilities: (*a*) cross-talk of the Rac/PAK pathway with c-Raf/MEK1/2/ERK1/2 and (*b*) involvement of integrins which are overexpressed and activated in schwannoma cells (6) and have been reported to lead to the activation of ERK1/2 via the FAK/Src/Ras pathway (29).

The Rac/PAK pathway is not involved in the increased basal activity of MEK1/2 and ERK1/2 in schwannoma cells. In basal conditions, c-Raf was only faintly phosphorylated at PAK phosphorylation site (Ser^{338}; Fig. 4*A, top*). MEK1/2, however, was phosphorylated at Ser^{298} (PAK phosphorylation site) in both Schwann and schwannoma cells, but no difference in the phosphorylation intensity was observed between these two cell types (Fig. 4*A, middle*). Additionally, PAK inhibitor IPA-3 did not decrease basal ERK1/2 activity. The ERK1/2 activity was instead potentiated, which possibly occurred due to cellular stress (Fig. 4*A, bottom*) as has been observed previously (30). Thus, it is unlikely that PAK contributes to the enhanced basal ERK1/2 activation.

Increased basal MEK1/2 and ERK1/2 activity in schwannoma cells is mediated via the integrin/FAK/src/Ras pathway. We thus looked at the FAK/Src/Ras pathway. Increased Ras-GTP levels, indicative for Ras activity, were detected by Ras pull-down analyses in serum-starved schwannoma cells compared with Schwann cells (Fig. 4*B*). To couple basal MEK1/2 activity to Ras and Src, we used H-Ras inhibitor farnesyl protein transferase inhibitor FTI-277 and selective Src family kinase inhibitor SU6656 (4 μmol/L). Both inhibitors decreased significantly basal p-MEK1/2 levels, suggesting Ras and Src to be involved in the pathway toward basal MEK1/2 activation (Fig. 4*C*).

FAK is overexpressed and displays strong basal activity in schwannoma cells. Focal adhesion kinase (FAK) is a tyrosine kinase that is activated after integrin-mediated attachment of the

cells to the extracellular matrix and plays an essential role in integrin signaling and tumorgenesis (31). Upon the interaction of integrins with the extracellular matrix, FAK is autophosphorylated at Y^{397}. If further phosphorylated by Src at Y^{925}, FAK is linked to the Ras/Raf/MEK1/2/ERK1/2 pathway (30), and at Y^{861}, its autophosphorylation is enhanced (32).

Overexpression and increased basal activity of FAK were observed in schwannoma cells compared with Schwann cells (Fig. 4*D*). FAK was strongly phosphorylated at Y^{397} (Fig. 4*D, second, third,* and *fourth panels*), Y^{861}, and Y^{925} (Fig. 4*D, second* and *third panels*) in schwannoma cells. The phosphorylation intensity of FAK at all sites investigated was not affected by PDGF-DD (Fig. 4*D, third panel*).

To further investigate the relationship between FAK activation, integrins, and basal ERK1/2 activity, we analyzed the cellular localization of p-ERK1/2 and p-FAK using immunofluorescence double labeling. p-ERK1/2 and p-FAK Y397 colocalize at focal adhesions in schwannoma cells (Fig. 4*D, fourth panel*), suggesting that the basal ERK activation is due to integrin-mediated activation of the FAK/Src/Ras pathway.

PDGFRβ-Mediated ERK1/2 Activation Employs PKC-Src-c-Raf and Involves Two Different Compartments

To define a specific mediator in the PDGFRβ-mediated signaling cascades toward ERK1/2 and AKT activation in schwannoma cells, we performed a dissection of these pathways by using a variety of different specific inhibitors. The specificity of signaling upon PDGF-DD stimulation was confirmed by using the PDGFRβ inhibitor AG1296 (20 and 40 μmol/L; Fig. 5*B*).

We first focused on 42/44 kDa bands. Ras often plays an essential role in the activation of the ERK1/2 via different mediators (33); however, the main pathways are either via direct coupling to c-Raf or via indirect c-Raf activation through the PI3K/phosphatidylinositol 3-phosphate–dependent kinase-1 (PDK1)/PKC cascade (34). The addition of PDGF-DD (100 ng/mL) for 3 minutes did not further enhance Ras activity (Fig. 5*A* and Supplementary Fig. S2*A*, compare *rows 1* and *2*), despite strong ERK1/2 activation at that time point (data not shown). Additionally, FTI-277 (30 μmol/L) did not inhibit PDGF-DD–mediated ERK1/2 activity (Fig. 5*B, top, row 9* and Supplementary Fig. S3, compare *rows 2* and *3*), suggesting that in schwannoma cells Ras is activated independently of PDGFRβ. The proper function of the FTI-277 is shown via Ras pull-down (Supplementary Fig. S2*A* and *B*).

We next investigated the involvement of PI3K, which acts either via Ras or via direct coupling to phosphorylated PDGFR (35), resulting in elevated phosphatidylinositol-3,4,5-trisphosphate levels, PKC activation via PDK1, and finally ERK1/2 activation. The nonsubtype-selective PI3K inhibitors wortmannin (300 nmol/L) and LY294002 (10 μmol/L; ref. 36) reduced PDGF-DD–mediated ERK1/2 activation by 40% to 60% (Fig. 5*B, top, columns 6* and *7*). In the PI3K-mediated cascade toward activation of ERK1/2, PKC can be one of the mediators. We assessed the role of PKC using the inhibitor of the classic and the novel PKC isoenzymes GF109203X (37) and by prolonged exposure of the cells to the PKC activator TPA (38). Both GF109203X (10 μmol/L) and TPA (100 nmol/L) strongly inhibited PDGF-DD–mediated ERK1/2 activation by ~60% and 40%, respectively (Fig. 5*B, top, columns 4* and *5*).

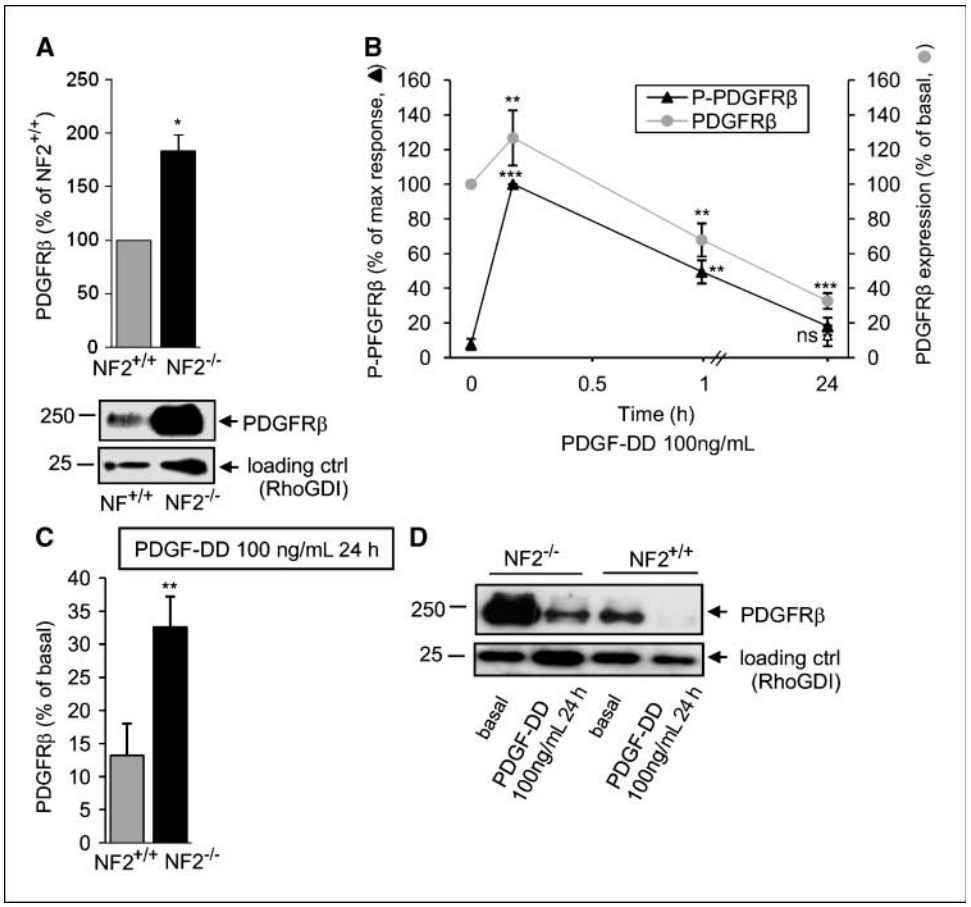

Figure 3. The expression, activation, and degradation of PDGFRβ in Schwann ($NF2^{+/+}$) and schwannoma ($NF2^{-/-}$) cells. *A,* PDGFRβ is overexpressed in schwannoma cells. Schwann and schwannoma cells were cultured in GFM and PDGFRβ expression estimated. *B* and *C,* the degradation and inactivation of PDGFRβ is postponed in schwannoma cells. *B,* schwannoma cells were serum starved for 24 h and stimulated with PDGF-DD (100 ng/mL) for the time indicated, and phosphorylation/activation and expression of PDGFRβ were estimated. *C* and *D,* Schwann and schwannoma cells were serum starved for 24 h and stimulated with 100 ng/mL PDGF-DD for 24 h, and the expression of PDGFRβ was estimated. Western blot method was used in all the experiments. *A,* data are normalized to $NF2^{+/+}$. *B,* data are normalized to basal level (nonstimulated cells) for PDGFRβ and to the maximum PDGF-DD stimulation (100%) for phosphorylated PDGFRβ. *C,* data are normalized to the basal level (nonstimulated cells). *Empty triangle in B,* basal level for 24 h stimulation. All data are corrected to loading control RhoGDI.

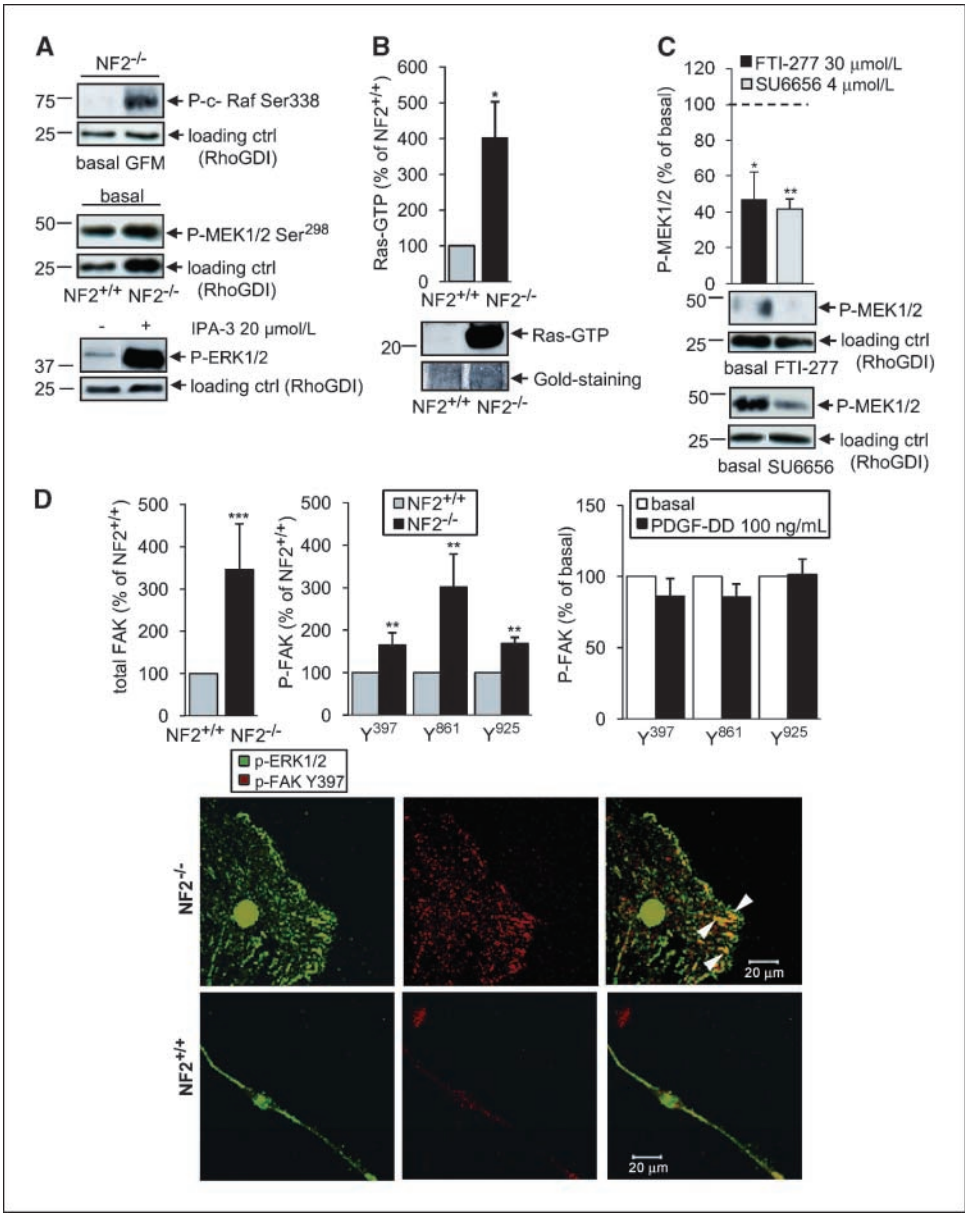

Figure 4. Dissection of the signaling pathway toward basal ERK1/2 activation in schwannoma cells. The following molecules were investigated: PAK (*A*) Ras (*B* and *C*), Src (*C*), and FAK (*D*). In all experiments, the cells were serum starved for 24 h, followed by stimulation for 10 min with complete medium (GFM; *A*) and 100 ng/mL PDGF-DD (*D, third panel*). Western blot method was used in all experiments but *D* (*fourth panel*), Ras pull-down was used in *B,* and immunocytochemistry in *D, fourth panel*. *A,* PAK is not involved in ERK1/2 activation in basal conditions. Schwannoma cells were starved for 24 h and stimulated with GFM for 10 min. The basal- and GFM- stimulated phosphorylation of c-Raf Ser^{338} (PAK phosphorylation site) and basal levels of phosphorylated MEK1/2 Ser^{298} (PAK phosphorylation site) in schwannoma cells were estimated by Western blot (*A, top* and *middle*). Cells were pretreated with the PAK inhibitor IPA-3 (20 μmol/L) for 10 min and lysed, and the levels of basal ERK1/2 were determined (*A, bottom*). *B,* Ras is strongly activated in schwannoma cells in serum-free conditions. Active Ras (Ras-GTP) levels in Schwann (NF2$^{+/+}$) and schwannoma (NF2$^{-/-}$) cells were estimated by Ras pull-down and Western blot after the cells were serum starved for 24 h. *C,* Ras and Src are involved in MEK1/2 activation in basal conditions. Cells were pretreated with farnesyl protein transferase inhibitor FTI-277 (30 μmol/L) and with Src inhibitor SU6656 (4 μmol/L) for 30 min, and the level of phosphorylated MEK1/2 was determined. *D,* FAK is overexpressed and strongly activated in schwannoma cells. FAK expression in Schwann (NF2$^{+/+}$) and schwannoma (NF2$^{-/-}$) cells was estimated by Western blot after the cells were serum starved for 24 h (*first panel*). FAK is strongly phosphorylated/activated in schwannoma cells (NF2$^{-/-}$) compared with Schwann cells (NF2$^{+/+}$). The cells were serum starved for 24 h, and the levels of phosphorylated/activated FAK (Y^{397}, Y^{861}, and Y^{925}) in Schwann and schwannoma cells were estimated by Western blot (*second panel*). Basal FAK activity is not further regulated by PDGF-DD. The cells were serum starved for 24 h and stimulated for 10 min with 100 ng/mL PDGF-DD. The basal- and PDGF-DD–stimulated levels of p-FAK (Y^{397}, Y^{861}, and Y^{925}) in schwannoma cells were estimated by Western blot (*third panel*). Phosphorylated ERK1/2 and p-FAK colocalize at focal adhesions in schwannoma cells. The colocalization of p-FAK with phosphorylated ERK1/2 in focal adhesions was performed after cells were serum starved for 24 h. *White arrowheads,* colocalizing p-ERK1/2 and p-FAK Y^{397} in the focal adhesions (*fourth panel*). *B* and *D* (*first and second panels*), data are normalized to NF2$^{+/+}$. *C* and *D* (*third panel*), data are normalized to the basal (nonstimulated cells). *Dotted lines in C,* noninhibited basal response and comparisons to noninhibited response (100%). All Western blot data are corrected to loading control RhoGDI.

Src family protein kinases interact with the ERK1/2 pathway via phosphorylation and activation of c-Raf or PKCδ (39). Our data show that PDGFRβ activation in schwannoma cells leads to the phosphorylation of c-Raf at the Src phosphorylation sites Y$^{340/341}$ (data not shown). We thus investigated the involvement of Src in PDGF-DD–mediated ERK1/2 activation using the selective Src family kinase inhibitor SU6656 (4 μmol/L) that strongly inhibited ERK1/2 activity (Fig. 5*B, top, column 8*).

Additionally, we explored the involvement of c-Raf using the specific inhibitor GW 5074 (5 μmol/L) that decreased ERK1/2 activity by 80% (Fig. 5*B, top, column 2*). PAK is not involved in PDGFRβ-mediated ERK1/2 activation in schwannoma cells, as PDGF-DD treatment did not lead to phosphorylation of either c-Raf at the PAK phosphorylation site (Ser^{338}) or MEK1/2 at the PAK phosphorylation site (Ser^{298}; Fig. 5*C, first* and *second panels*). Moreover PAK inhibitor IPA-3 displayed no effect on PDGF-DD–stimulated activity of MEK1/2 and ERK1/2 (Fig. 5*C, third panel, lines 1* and *3*) excluding PAK as a mediator of this ERK1/2 cascade activation.

Using the same inhibitors as for investigation of the ERK1/2 pathway, we show that PDGF-DD–mediated AKT activation follows the traditional pathway engaging PI3K since the inhibitors wortmannin (300 nmol/L) and LY294002 (10 μmol/L) strongly inhibited AKT phosphorylation (Ser^{473}; Fig. 5*B, bottom, columns 7* and *8*).

Thus, PDGFRβ-mediated ERK1/2 activation displayed at the 42/44 kDa level is independent of Ras and PAK but uses PI3K-PKC-Src-c-Raf–dependent pathway and cross-talk with AKT at the level of PI3K.

Despite similarities, such as involvement of c-Raf, PKC, and Src (Fig. 5*B*, compare *top* and *middle, columns 2, 4, 5,* and *8*) and bypassing Ras (Fig. 5*B*, compare *top* and *middle, column 9*) the activity of the ERK1/2 pathway at 42/44 kDa and 300 kDa differ regarding the involvement of MEK1/2, PI3K (Fig. 5*B*, compare *top* and *middle, columns 3, 6,* and *7*), and PAK (Fig. 5*C, third panel, lines 2* and *3*). In contrast to ERK1/2 activation at the 42/44 kDa level that depends on PI3K and MEK1/2, the 300-kDa bands are independent from those kinases. The engagement of PAK also differs because PDGF-DD mediated ERK1/2 activity at the 300-kDa level is almost completely inhibited by the PAK inhibitor IPA-3 (Fig. 5*C third panel, line 2*) whereas this, at 42/44 kDa, was unaffected (Fig. 5*C, third panel, line 3*). Additional data obtained by immunocytochemistry showed that IPA-3 completely abolished the ERK1/2 activity in focal adhesions and membrane and also eliminated the p-ERK1/2 clustering in the dot-like structures in the cytosol. However, the total ERK1/2 activity in the cytosol was unaffected, thus confirming Western blot data and suggesting PAK acting as a scaffold in a complex containing ERK (Fig. 5*C, fourth*

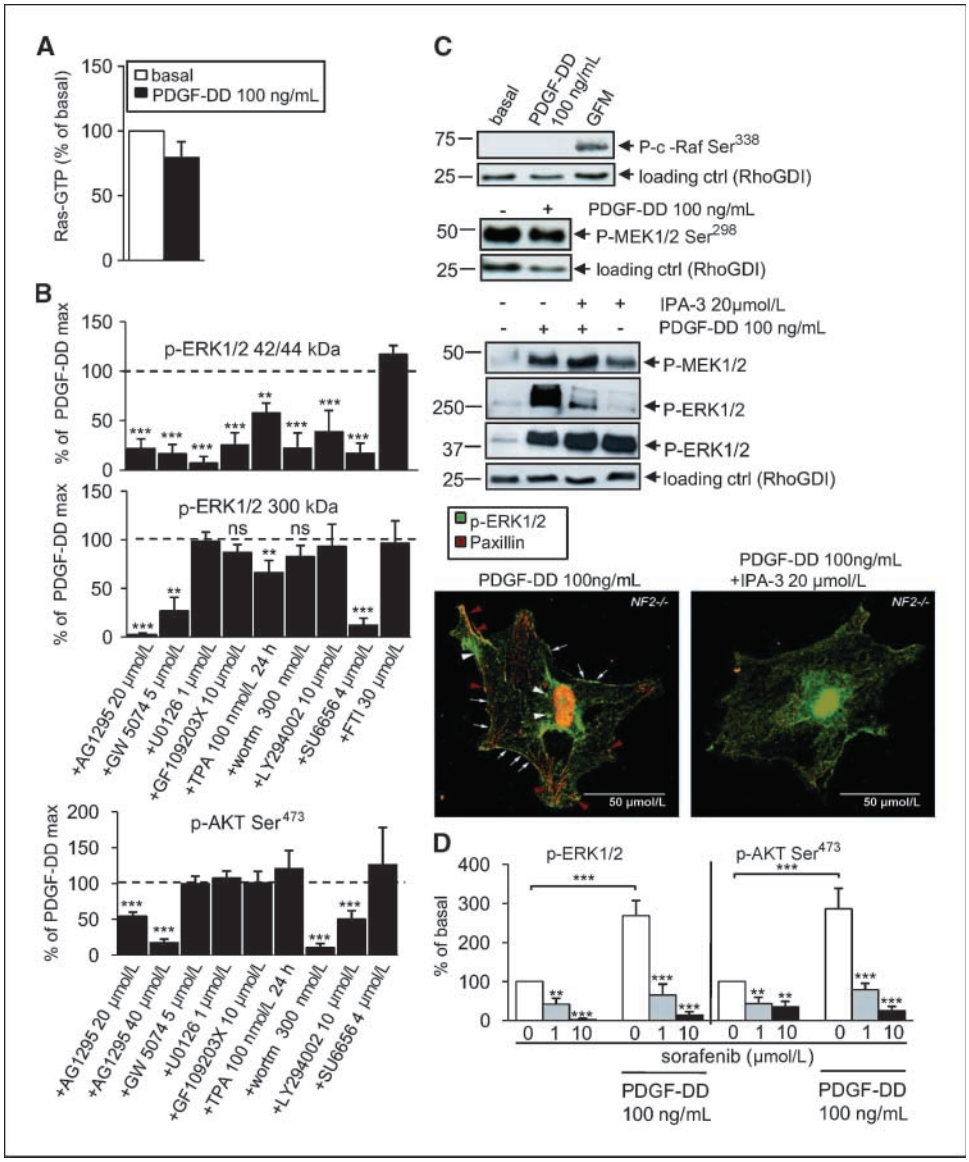

Figure 5. The dissection of the PDGF-DD–mediated cascades in schwannoma cells. The ERK1/2 signaling pathway was investigated by analyzing the involvement of Ras (*A* and *B*); MEK1/2, PKC, PI3K, and Src (*B*); PDGFRβ and c-Raf (*B* and *D*); and PAK (*C*). The AKT signaling pathway was investigated by analyzing the involvement of MEK1/2, PKC, PI3K, and Src (*B*) and PDGFRβ and c-Raf (*B* and *D*). In all experiments, the cells were serum starved for 24 h before the stimulation with PDGF-DD (100 ng/mL; *A–D*) or complete medium (GFM; *C, first panel*) for 10 min (*A*; 3 min). The detection of phosphorylated/activated proteins was performed by Western blotting in all experiments but *C* (*fourth panel*), where immunocytochemistry method was used. In *A*, Ras pull-down was performed before Western blotting. In *B*, the cells were pretreated with PDGFβ inhibitor (AG1296), c-Raf inhibitor (GW5074), MEK1/2 inhibitor (U0126), PKC inhibitor (GF109203X), or with PKC activator TPA, PI3K inhibitors (Wortmannin and LY294002), Src inhibitor (SU6656), and farnesyl protein transferase inhibitor (FTI-277) before stimulation. *C,* coupling of PAK to ERK1/2 cascade was estimated using anti-phosphorylated c-Raf Ser^{338} (*first panel*), anti–p-MEK1/2 Ser^{298} (*second panel*) antibodies, and PAK inhibitor IPA-3 (20 μmol/L; *third and fourth panels*). *Fourth panel,* the cells were stimulated with PDGF-DD (100 ng/mL) for 10 min with and without IPA-3 (20 μmol/L) and stained for p-ERK1/2 (*green*) and paxillin (a focal adhesion marker, *red*). *White arrowheads,* dot-like structures in the cytosol; *red arrowheads,* focal adhesions (visualized by paxillin staining in red); *white arrows,* membrane staining. *D,* cells were pretreated with sorafenib (Bay 43-9006) before the stimulation. In all the experiments, the inhibitors were added 30 min before the stimulation and TPA was added 24 h before the stimulation and IPA3 for 10 min. *Dotted lines* in *B,* noninhibited PDGF-DD response and comparisons to noninhibited response (100%). *D,* data are normalized to the basal levels (nonstimulated cells). All Western blot data are corrected to loading control RhoGDI.

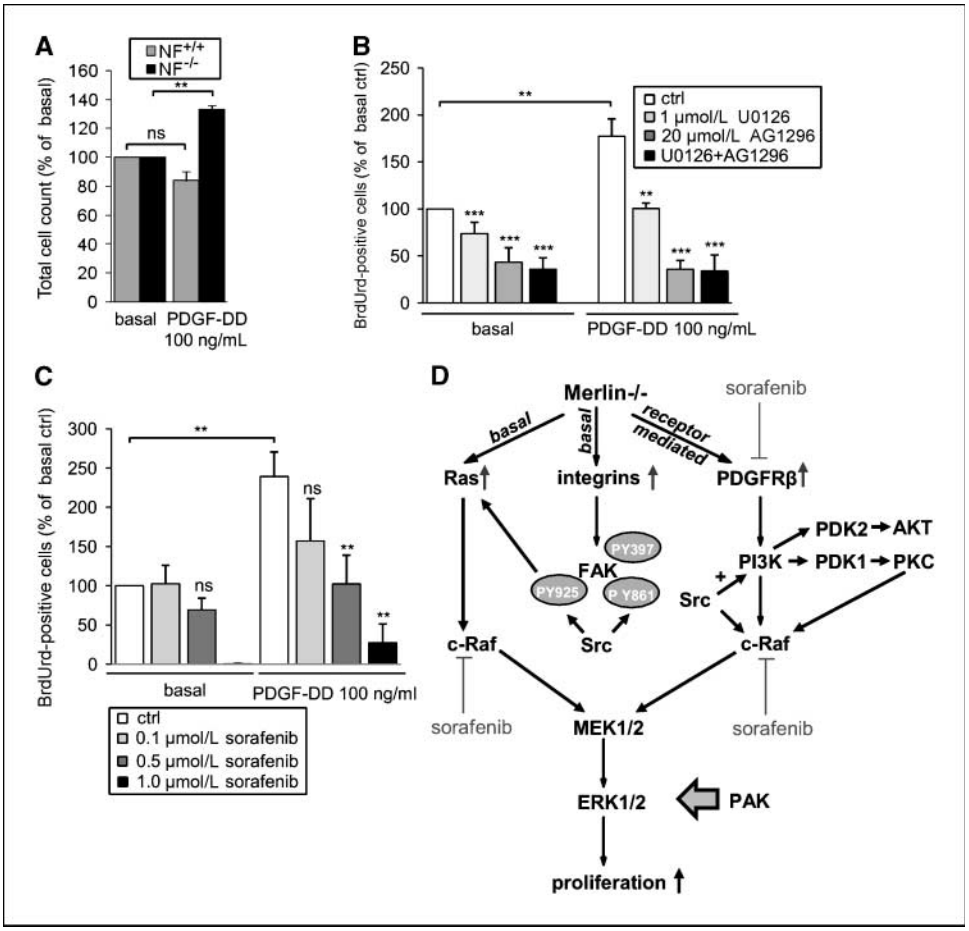

Figure 6. Signaling pathways involved in the enhanced proliferation of schwannoma cells. *A,* Schwann ($NF2^{+/+}$) and schwannoma cells($NF2^{-/-}$) were cultured for 72 h with or without PDGF-DD. Total cell amount was estimated by nuclear staining with 5 μg/mL Hoechst 33342 and cell counting. *B* and *C,* schwannoma cells were incubated with U0126 (MEK1/2 inhibitor), AG1296 (PDGFRβ inhibitor), and U0126 together with AG1296 (*B*) and sorafenib (PDGFRβ and Raf inhibitor; *C*) with and without PDGF-DD for 72 h. BrdUrd (10 μmol/L) was added during the last 24 h of the experiment. The amount of proliferating cells (BrdUrd-positive) was assessed by cell counting. In all experiments, the data are normalized to the basal level (nonstimulated cells). *D,* signaling pathways targeted by sorafenib in schwannoma cells. Merlin deficiency leads to the activation of Ras, overexpression and activation of integrins, and overexpression and postponed degradation of PDGFRβ. Ras and integrins trigger basal ERK1/2 activity via FAK, which is strongly overexpressed and phosphorylated/activated by Src. Basal ERK1/2 activity is further potentiated via PDGFRβ-mediated PI3K/PKC/Src/c-Raf/MEK1/2 and cascade. PAK acts as a scaffold in a complex containing active ERK1/2.

panel). Thus, our data indicate that PDGF-DD–mediated ERK1/2 activation at the 300-kDa level engages c-Raf, PKC, src, and PAK and localizes to the different cellular compartments than active ERK1/2 observed at the 42/44 kDa level.

In summary, we found two major mechanisms converging toward ERK1/2 activation in schwannoma cells: (*a*) basal activation via integrins/src/FAK/Ras and (*b*) PDGFRβ-mediated via the PI3K-PKC-c-Raf and PKC-PAK-c-Raf pathways were the first mentioned cross talk with and strongly activate AKT (Fig. 6*D*).

We thus chose sorafenib (1 and 10 μmol/L), an inhibitor of PDGFR and c-Raf (Fig. 6*D*) already used in clinic, which efficiently inhibited both basal- and PDGF-DD–stimulated ERK1/2 and AKT activity (Fig. 5*D*), suggesting that this compound has a potential therapeutic effect on schwannoma.

PDGFRβ Induces Enhanced Cell Proliferation, but not Adhesion, via ERK1/2 in Schwannoma Cells

We next assessed the functional role of PDGFRβ-mediated ERK1/2 activation in schwannoma cells.

Adhesion. First, we performed an adhesion assay (6) where cells were cultured in three different conditions: DMEM only, DMEM with 100 ng/mL PDGF-DD, and complete medium (GFM). Only GFM but not PDFG-DD alone induced schwannoma cell adhesion (data not shown); thus, it is unlikely that PDGFRβ alone play a role in this process.

Proliferation. We have previously shown that schwannoma cells display an increased proliferation rate compared with Schwann cells (40). As PDGF is a potent growth factor in several cell types, we tested its mitogenic potency in our *in vitro* model. The addition of 100 ng/mL PDGF-DD for 72 hours resulted in an increase of total cell number (determined by Hoechst 33342 staining of the nucleus) by ~40% in schwannoma cells, whereas no mitogenic effect on Schwann cells was detected (Fig. 6*A*) under our culture conditions. Additional experiments measuring BrdUrd incorporation revealed that schwannoma cells displayed basal proliferation activity, which was strongly potentiated by PDGF-DD by ~80% (Fig. 6*B* and *C*), indicating that PDGF-DD is a potent mitogen for human primary schwannoma cells. Both MEK1/2 and PDGFR inhibitors U0126 (1 μmol/L) and AG1296 (20 μmol/L), respectively, strongly reduced PDGF-DD–mediated as well basal cell proliferation (Fig. 6*B*), suggesting that the ERK1/2 pathway is involved in PDGFRβ-mediated proliferation in schwannoma cells. Next, we tested sorafenib (0.1, 0.5, and 1 μmol/L), a PDGFR and c-Raf inhibitor that is currently approved for clinical use in advanced RCC. Interestingly, 0.5 μmol/L sorafenib effectively inhibited PDGF-DD but not basal and 1 μmol/L inhibited both PDGF-DD–mediated and basal proliferation in schwannoma cells (Fig. 6*C*), suggesting that this component could be used for schwannoma treatment.

Discussion

We show strong and prolonged ERK1/2 pathway activation in human primary schwannoma cells compared with primary Schwann cells. PDGFRβ is strongly overexpressed in human primary schwannoma cells in agreement with a previous observation in human schwannoma tissue (18). Insulin and β

heregulin activate ERK1/2 only weakly, even when used at high concentrations. FGFa and EGF fail to activate ERK1/2. Additionally, the expression levels of ErbB2 and ErbB3 receptors are equal in human schwannoma and Schwann cells. EGFR is present in the rat schwannoma cell line RT4 (data not shown), but not in human primary Schwann and schwannoma cells. Thus, PDGFRβ is a crucial receptor signaling through ERK1/2 pathway in human schwannoma.

In addition to the activation of the ERK1/2 pathway, PDGF-DD also evokes a strong and prolonged AKT response in schwannoma cells compared with Schwann cells. Although PDGFRβ is important for the activation of the AKT pathway, as shown here, we cannot exclude that, in different physiologic milieu, other growth factors could also be involved in activation of this pathway.

PDGFRβ displays a postponed degradation in schwannoma cells compared with Schwann cells, in agreement with a previous study on human schwannoma cell line HEI193 (18). The receptor activity is prolonged and, 1 hour after stimulation, decreased only by 50% of maximum response. The kinetics of PDGFR deactivation is usually much faster, as shown in fibroblasts, where already 20 minutes after stimulation the activity dropped by 75% (41). Our data suggest that one of functions of merlin is to regulate the receptor activity. PDGFRβ phosphorylation/activity display the same pattern as MEK1/2 and ERK1/2 activity, but diverge from AKT, which exhibit strong activity even 24 hours after stimulation. Thus, in schwannoma cells, AKT activation is regulated not only at the PDGFRβ level but possibly also by positive feedback mechanisms downstream of the receptor, e.g., saturation of PI3K activity (41), prolongation of signaling in endosomes (42), or activation of phosphatase inhibitors (43). These human data extend the observations made in the rat schwannoma cell line RT4 and in a mouse $NF2^{-/-}$ Schwann cell line, where receptor expression and function were not affected by merlin (16). In addition to strong and long-lasting PDGF-DD–mediated MEK1/2 and ERK1/2 activity, schwannoma cells display stronger basal activity of these kinases compared with Schwann cells. This could involve either Rac/PAK or integrin-mediated pathways. PAK can be excluded as an activator of ERK1/2 at 42/44kDa level, which is the main ERK1/2 band in basal conditions, as c-Raf is not phosphorylated at its PAK phosphorylation site (Ser^{338}) and analysis of the PAK-dependent phosphorylation site on MEK1/2 (Ser^{298}) shows that schwannoma and Schwann cells display similar phosphorylation levels. Also, the PAK inhibitor IPA-3 inhibited neither basal- nor PDGF-DD–stimulated MEK1/2 and ERK1/2 activity. This is an unexpected finding because the Rac1/PAK pathway is strongly up-regulated in schwannoma cells (8) and PAK is known to act as a scaffold to enhance ERK1/2 activity (44). However, we found instead that ERK1/2 activity at the 300-kDa level, prominent after PDGF stimulation, is dependent from PAK that likely acts as a scaffold. Moreover, the activation of the ERK1/2 at the 300-kDa level displays also other differences from this at 42/44 kDa, as it bypasses PI3K and MEK1/2. A potential explanation could be hidden binding sites for those inhibitors caused by complex formation. Immunocytochemistry also show the differential distribution of p-ERK1/2 in schwannoma cells (nucleus, cytosol, membrane, and focal adhesions). Our data thus suggest that PDGF-DD mediates the activation of ERK1/2 in different cellular compartments which display different molecular background. We next tested the role of integrins that are up-regulated in schwannoma (6) and may activate ERK1/2 via the FAK/src/Ras pathway (29). We detected enhanced basal activity of Ras, MEK1/2, and ERK1/2 and increased expression and activation of FAK in schwannoma cells. Additionally, p-FAK colocalizes with p-ERK1/2 in focal adhesions. Moreover, blocking of Ras and Src inhibit basal MEK1/2 activity. Taken together, these results indicate that integrins are likely to contribute to ERK1/2 activation in schwannoma cells via the FAK/src/Ras pathway under basal conditions. We think that in basal conditions schwannoma cells display activation of the integrin/FAK/Src cascade, as well as increased levels of active Ras, which, upon coupling to p-FAK (Y^{925}), leads to activation of ERK1/2.

As the stimulation of PDGFRβ strongly potentiates ERK1/2 and AKT activity, we consider that this receptor and its downstream signaling pathways is important for schwannoma development. To define a potential therapeutic target for schwannoma treatment, we performed a dissection of the cascades downstream of PDGFRβ in addition to basal activation. Our data suggest cooperation between PI3K, PKC, and Src in PDGF-DD–mediated ERK1/2 activation. Although Ras is strongly activated in schwannoma cells and implicated in basal signaling toward ERK1/2 activation, it is not further activated by PDGF-DD and is not involved in the PDGFRβ-mediated pathway. This could be explained by a possible uncoupling of Ras from the receptor. Different Ras isoforms localize to distinct microdomains within plasma membrane and different intracellular compartments leading to diverse signal outputs despite interaction with similar activators and effectors (45). Ras insensitivity to PDGF-DD could also be explained by either saturated basal activity of Ras or a negative feedback from basal ERK1/2 to Grb2-Sos (Ras-GEF; ref. 46). Our data somehow contradicts previous findings, showing Ras involved in PDGFRβ-mediated ERK1/2 activation (16). This discrepancy may be down to the use of rat schwannoma cell line caused by different mutation and displaying malignant properties by Morrison and colleagues, whereas we focused our study on primary human schwannoma.

We show that PDGF-DD engages different pathways to activate ERK1/2 that is localized to different intracellular compartments and detected at different molecular weight levels by Western blot. The p-ERK1/2 pathway at 42/44 kDa (cytosol) favors a model in which c-Raf is activated by Src and PKC, where the later is activated by PI3K (via PDK1), which directly binds to phosphorylated/activated PDGFRβ (Fig. 6*D*; refs. 47, 48). PI3K acts also as a convergence point to the activation of AKT (Fig. 6*D*). The p-ERK1/2 pathway at 300-kDa level (focal adhesions) engages c-Raf, PKC, Src, and PAK. Our data thus fit to previous observations showing that ERK1/2 activity is tightly regulated by merlin (17) and involved in rat Schwann cells dedifferentiation (13) and integrin-mediated cell motility and adhesion (14), which is dramatically disregulated in merlin-deficient schwannoma cells (6).

Whereas transient ERK1/2 activity is important for normal cell function, a strong and long-lasting ERK1/2 activation can be mitogenic (49, 50). We show increased proliferation of schwannoma cells upon stimulation with PDGF-DD, whereas no effects were observed in Schwann cells. This could be explained either by the short and weak ERK1/2 activity in those cells or a requirement for additional factors in the culture medium, such as insulin-like growth factors (51). Inhibition of MEK1/2 decreases PDGF-DD–mediated proliferation to basal levels, suggesting that ERK1/2 pathway is involved in this process. Additionally, both MEK1/2 and PDGFRβ inhibition significantly inhibited basal cell proliferation, suggesting that both the integrin/FAK/src/Ras cascade and PDGFRβ-mediated signaling, possibly via autocrine mechanisms, are involved in schwannoma cell proliferation.

Based on this evidence, we consider PDGFRβ-mediated signaling to be involved in schwannoma development. Additionally, the integrin-mediated FAK/src/Ras cascade contributes to basal ERK1/2 activity, thereby potentiating the PDGFRβ-specific pathway (Fig. 6*D*; ref. 16).

Because different pathways are involved in schwannoma cell proliferation, we suggest that a combined therapy targeting different proteins might be appropriate for treating schwannoma. Promising therapeutic agent include sorafenib, a PDGFR and Raf inhibitor already approved for use in patients with advanced RCC, as it inhibits efficiently both basal and PDGF-DD–mediated ERK1/2 and AKT activation and proliferation in human primary schwannoma cells.

Disclosure of Potential Conflicts of Interest

No potential conflicts of interest were disclosed.

Acknowledgments

Received 10/11/2007; revised 3/4/2008; accepted 4/9/2008.

Grant support: Children's Tumor Foundation and Peninsula College of Medicine and Dentistry.

The costs of publication of this article were defrayed in part by the payment of page charges. This article must therefore be hereby marked *advertisement* in accordance with 18 U.S.C. Section 1734 solely to indicate this fact.

We thank Prof. Jyrki Kukkonen (University of Helsinki) for GF109203X, LY294002, SU6656, U0126, and wortmannin, Bayer Pharmaceuticals for sorafenib (BAY 43-9006), and Dr. Jeffrey R Peterson (Fox Chase Cancer Center) for IPA-3.

References

1. McClatchey AI, Giovannini M. Membrane organization and tumorigenesis-the NF2 tumor suppressor, Merlin. Genes Dev 2005;19:2265–77.
2. Rouleau GA, Merel P, Lutchman M, et al. Alteration in a new gene encoding a putative membrane-organizing protein causes neuro-fibromatosis type 2 (see comments). Nature 1993;363:515–21.
3. Trofatter JA, MacCollin MM, Rutter JL, et al. A novel moesin-, ezrin-, radixin-like gene is a candidate for the neurofibromatosis 2 tumor suppressor. Cell 1993;75:826.
4. Bretscher A, Edwards K, Fehon RG. ERM proteins and merlin: integrators at the cell cortex. Nat Rev Mol Cell Biol 2002;3:586–99.
5. Utermark T, Kaempchen K, Antoniadis G, Hanemann CO. Reduced apoptosis rates in human schwannomas. Brain Pathol 2005;15:17–22.
6. Utermark T, Kaempchen K, Hanemann CO. Pathological adhesion of primary human schwannoma cells is dependent on altered expression of integrins. Brain Pathol 2003;13:352–63.
7. Flaiz C, Utermark T, Parkinson DB, Poetsch A, Hanemann CO. Impaired intercellular adhesion and immature adherens junctions in merlin-deficient human primary schwannoma cells. Glia 2008;56:506–15.
8. Kaempchen K, Mielke K, Utermark T, Langmesser S, Hanemann CO. Upregulation of the Rac1/JNK signaling pathway in primary human schwannoma cells. Hum Mol Genet 2003;12:1211–21.
9. Flaiz C, Kaempchen K, Matthies C, Hanemann CO. Actin-rich protrusions and nonlocalized GTPase activation in merlin-deficient schwannomas. J Neuropathol Exp Neurol 2007;66:608–16.
10. Kissil JL, Wilker EW, Johnson KC, Eckman MS, Yaffe MB, Jacks T. Merlin, the product of the Nf2 tumor suppressor gene, is an inhibitor of the p21-activated kinase, Pak1. Mol Cell 2003;12:841–9.
11. Hirokawa Y, Tikoo A, Huynh J, et al. A clue to the therapy of neurofibromatosis type 2: NF2/merlin is a PAK1 inhibitor. Cancer J 2004;10:20–6.
12. Pelton PD, Sherman LS, Rizvi TA, et al. Ruffling membrane, stress fiber, cell spreading and proliferation abnormalities in human schwannoma cells. Oncogene 1998;17:2195–209.
13. Harrisingh MC, Perez-Nadales E, Parkinson DB, Malcolm DS, Mudge AW, Lloyd AC. The Ras/Raf/ERK signalling pathway drives Schwann cell dedifferentiation. EMBO J 2004;23:3061–71.
14. Sawhney RS, Cookson MM, Omar Y, Hauser J, Brattain MG. Integrin α2-mediated ERK and calpain activation play a critical role in cell adhesion and motility via focal adhesion kinase signaling: identification of a novel signaling pathway. J Biol Chem 2006;281:8497–510.
15. Meloche S, Pouyssegur J. The ERK1/2 mitogen-activated protein kinase pathway as a master regulator of the G1- to S-phase transition. Oncogene 2007;26:3227–39.
16. Morrison H, Sperka T, Manent J, Giovannini M, Ponta H, Herrlich P. Merlin/neurofibromatosis type 2 suppresses growth by inhibiting the activation of Ras and Rac. Cancer Res 2007;67:520–7.
17. Lim JY, Kim H, Jeun SS, Kang SG, Lee KJ. Merlin inhibits growth hormone-regulated Raf-ERKs pathways by binding to Grb2 protein. Biochem Biophys Res Commun 2006;340:1151–7.
18. Fraenzer JT, Pan H, Minimo L, Jr., Smith GM, Knauer D, Hung G. Overexpression of the NF2 gene inhibits schwannoma cell proliferation through promoting PDGFR degradation. Int J Oncol 2003;23:1493–500.
19. Rong R, Tang X, Gutmann DH, Ye K. Neurofibromatosis 2 (NF2) tumor suppressor merlin inhibits phosphatidylinositol 3-kinase through binding to PIKE-L. Proc Natl Acad Sci U S A 2004;101:18200–5.
20. Li Y, Tennekoon GI, Birnbaum M, Marchionni MA, Rutkowski JL. Neuregulin signaling through a PI3K/Akt/Bad pathway in Schwann cell survival. Mol Cell Neurosci 2001;17:761–7.
21. Meier F, Schittek B, Busch S, et al. The RAS/RAF/MEK/ERK and PI3K/AKT signaling pathways present molecular targets for the effective treatment of advanced melanoma. Front Biosci 2005;10:2986–3001.
22. Heldin CH, Westermark B. Mechanism of action and *in vivo* role of platelet-derived growth factor. Physiol Rev 1999;79:1283–316.
23. Escudier B, Eisen T, Stadler WM, et al. Sorafenib in advanced clear-cell renal-cell carcinoma. N Engl J Med 2007;356:125–34.
24. Hanemann CO, Rosenbaum C, Kupfer S, Wosch S, Stoegbauer F, Mueller HW. Improved culture methods to expand Schwann cells with altered growth behaviour from CMT1A patients. GLIA 1998;23:89–98.
25. Rosenbaum C, Kluwe L, Mautner VF, Friedrich RE, Mueller HW, Hanemann CO. Isolation and characterization of Schwann cells from neurofibromatosis type 2 patients. Neurobiol Dis 1998;5:55–64.
26. National Institutes of Health Consensus Development Conference Statement on Acoustic Neuroma, December 11-13, 1991. The Consensus Development Panel. Arch Neurol 1994;51:201–7.
27. Hanemann CO, Bartelt-Kirbach B, Diebold R, Kampchen K, Langmesser S, Utermark T. Differential gene expression between human schwannoma and control Schwann cells. Neuropathol Appl Neurobiol 2006;32:605–14.
28. Milner R, Wilby M, Nishimura S, et al. Division of labor of Schwann cell integrins during migration on peripheral nerve extracellular matrix ligands. Dev Biol 1997;185:215–28.
29. Schlaepfer DD, Hunter T. Focal adhesion kinase overexpression enhances ras-dependent integrin signaling to ERK2/mitogen-activated protein kinase through interactions with and activation of c-Src. J Biol Chem 1997;272:13189–95.
30. Deacon SW, Beeser A, Fukui JA, et al. An isoform-selective, small-molecule inhibitor targets the autoregulatory mechanism of p21-activated kinase. Chem Biol 2008;15:322–31.
31. Hehlgans S, Haase M, Cordes N. Signaling via integrins: implications for cell survival and anticancer strategies. Biochim Biophys Acta 2007;1775:163–80.
32. Leu TH, Maa MC. Tyr-863 phosphorylation enhances focal adhesion kinase autophosphorylation at Tyr-397. Oncogene 2002;21:6992–7000.
33. Bos JL. All in the family? New insights and questions regarding interconnectivity of Ras, Rap1 and Ral. EMBO J 1998;17:6776–82.
34. Le Good JA, Ziegler WH, Parekh DB, Alessi DR, Cohen P, Parker PJ. Protein kinase C isotypes controlled by phosphoinositide 3-kinase through the protein kinase PDK1. Science 1998;281:2042–5.
35. Wymann MP, Zvelebil M, Laffargue M. Phosphoinositide 3-kinase signalling-which way to target? Trends Pharmacol Sci 2003;24:366–76.
36. Vlahos CJ, Matter WF, Hui KY, Brown RF. A specific inhibitor of phosphatidylinositol 3-kinase, 2-(4-morpholinyl)-8-phenyl-4H-1-benzopyran-4-one (LY294002). J Biol Chem 1994;269:5241–8.
37. Toullec D, Pianetti P, Coste H, et al. The bisindolylmaleimide GF 109203X is a potent and selective inhibitor of protein kinase C. J Biol Chem 1991;266:15771–81.
38. Bindels RJ, Dempster JA, Ramakers PL, Willems PH, van Os CH. Effect of protein kinase C activation and down-regulation on active calcium transport. Kidney Int 1993;43:295–300.
39. Steinberg SF. Distinctive activation mechanisms and functions for protein kinase Cdelta. Biochem J 2004;384:449–59.
40. Schulze KM, Hanemann CO, Muller HW, Hanenberg H. Transduction of wild-type merlin into human schwannoma cells decreases schwannoma cell growth and induces apoptosis. Hum Mol Genet 2002;11:69–76.
41. Park CS, Schneider IC, Haugh JM. Kinetic analysis of platelet-derived growth factor receptor/phosphoinositide 3-kinase/Akt signaling in fibroblasts. J Biol Chem 2003;278:37064–72.
42. Haugh JM, Lauffenburger DA. Analysis of receptor internalization as a mechanism for modulating signal transduction. J Theor Biol 1998;195:187–218.
43. Heinrich R, Neel BG, Rapoport TA. Mathematical models of protein kinase signal transduction. Mol Cell 2002;9:957–70.
44. Beeser A, Jaffer ZM, Hofmann C, Chernoff J. Role of group A p21-activated kinases in activation of extracellular-regulated kinase by growth factors. J Biol Chem 2005;280:36609–15.
45. Hancock JF. Ras proteins: different signals from different locations. Nat Rev Mol Cell Biol 2003;4:373–84.
46. Dong C, Waters SB, Holt KH, Pessin JE. SOS phosphorylation and disassociation of the Grb2-SOS complex by the ERK and JNK signaling pathways. J Biol Chem 1996;271:6328–32.
47. Chong H, Vikis HG, Guan KL. Mechanisms of regulating the Raf kinase family. Cell Signal 2003;15:463–9.
48. Tallquist M, Kazlauskas A. PDGF signaling in cells and mice. Cytokine Growth Factor Rev 2004;15:205–13.
49. Roovers K, Assoian RK. Integrating the MAP kinase signal into the G1 phase cell cycle machinery. Bioessays 2000;22:818–26.
50. Pouyssegur J, Volmat V, Lenormand P. Fidelity and spatio-temporal control in MAP kinase (ERKs) signalling. Biochem Pharmacol 2002;64:755–63.
51. Stewart HJ, Bradke F, Tabernero A, Morrell D, Jessen KR, Mirsky R. Regulation of rat Schwann cell Po expression and DNA synthesis by insulin-like growth factors *in vitro*. Eur J Neurosci 1996;8:553–64.

Dissecting and Targeting the Growth Factor–Dependent and Growth Factor –Independent Extracellular Signal-Regulated Kinase Pathway in Human Schwannoma

Sylwia Ammoun, Christine Flaiz, Natalia Ristic, et al.

Cancer Res 2008;68:5236-5245.